Biophysical Journal Volume 71 October 1996 1920–1933

Affinity and Structure of Complexes of Tropomyosin and Caldesmon Domains

Eric J. Hnath,* C.-L. Albert Wang,# Pia A. J. Huber,§ Steve B. Marston,§ and George N. Phillips, Jr.*
*Department of Biochemistry and Cell Biology, W. M. Keck Center for Computational Biology, Rice University, Houston, Texas 77005 USA; #Muscle Research Group, Boston Biomedical Research Institute, Boston, Massachusetts 02114 USA; and §Imperial College School of Medicine at the National Heart and Lung Institute, Dovehouse Street, London SW3 6LY England

ABSTRACT The interaction of caldesmon domains with tropomyosin has been studied using x-ray crystallography and an optical biosensor. Only whole caldesmon and the carboxyl-terminal domain of caldesmon (CaD-4, chicken gizzard residues 597–756) bound to tropomyosin with greater than millimolar affinity at 100 and 150 mM salt. Under these conditions the affinities of whole caldesmon and CaD-4 were both in the micromolar range. Data from the x-ray studies showed that whole caldesmon bound to tropomyosin in several places, with the region of tightest interaction being at tropomyosin residues 70–100 and/or 230–260. Studies with CaD-4 revealed that this region corresponded to the strong binding site seen with whole caldesmon. Weaker association of other regions of caldesmon to tropomyosin residues 180–210 and 5–50 was also observed. The results suggest that the carboxyl-terminus of caldesmon binds tightly to tropomyosin and that other regions of caldesmon may interact with tropomyosin tightly only when they are held close to tropomyosin by the carboxyl-terminal domain. Four models are presented to show the possible interactions of caldesmon with tropomyosin.

INTRODUCTION

Regulation of smooth muscle contraction is primarily mediated by phosphorylation of myosin light chains by myosin light chain kinase complexed with Ca^{+2}-calmodulin (Allen and Walsh, 1994). A number of experiments, however, indicate that the phosphorylation of myosin cannot account for all of the observed behaviors of smooth muscle (Allen and Walsh, 1994). The observation of in vitro calcium-regulated inhibition of actomyosin ATPase by smooth muscle thin filaments led to the suggestion that smooth muscle may contain a thin filament regulatory system similar to the troponin system found in all striated muscle (Hemric et al., 1993; Marston and Smith, 1985).

Caldesmon, identified as a possible thin filament regulatory switch in smooth muscle (Sobue et al., 1981), is an 89-kDa elongated protein that binds tightly to myosin, actin, tropomyosin, and several calcium-binding proteins, including calmodulin (Marston and Redwood, 1991). In reconstituted systems caldesmon inhibits the actin-activated ATPase activity of myosin by several different mechanisms: 1) inhibition of weak cross-bridge binding between actin and myosin; 2) cross-linking of actin and myosin, which can impede filament movement; and 3) tropomyosin-dependent inhibition (Kraft et al., 1995; Marston et al., 1994a). All of these inhibitions are diminished by the binding of Ca^{+2}/calmodulin to caldesmon, which reduces the affinity of caldesmon for actin, tropomyosin, and myosin (Watson et al., 1990a).

Received for publication 16 April 1996 and in final form 8 July 1996.

Address reprint requests to George Phillips, Department of Biochemistry and Cell Biology, Rice University, 6100 Main St., Houston, TX 77005. Tel.: 713-527-4910; E-mail: georgep@bioc.rice.edu.

0006-3495/96/10/1920/14 $2.00

Caldesmon probably plays a significant role in the thin filament calcium regulation of smooth muscles, because antibodies to caldesmon abolish calcium sensitivity of muscle actin-activated myosin ATPase (Marston et al., 1988). Further evidence of caldesmon's importance comes from studies where thin filaments were reconstituted with physiological ratios of caldesmon, tropomyosin, and actin (2:1:14) (Dabrowska et al., 1985; Smith et al., 1987). These filaments are calcium regulated in the presence of calmodulin. Other studies using caldesmon fragments suggest that caldesmon regulates contraction in some smooth muscle cells by providing a basal resting inhibition of vascular tone (Katsuyama et al., 1992).

Many studies using segments of caldesmon have been conducted in an attempt to define the functional domains of caldesmon. Several binding sites have been identified in vitro for actin, myosin, calmodulin, and tropomyosin. It has been suggested that caldesmon is composed of four domains joined by mainly unstructured polypeptide regions (Marston and Redwood, 1991). Domain 1 is at the amino terminus and is believed to bind to myosin. Domain 2 is known as the central repeating helical region and is absent in nonmuscle isoforms. Domain 3 contains a region with homology to troponin T. Domain 4, the C-terminal part of caldesmon, is known to include most of the regulatory properties of the entire molecule and includes the binding sites for actin, calmodulin, myosin, and tropomyosin. The C-terminal domain has been further subdivided into two pieces, domain 4a (chicken gizzard residues 600–657) and domain 4b (residues 658–756) (Redwood and Marston, 1993).

Most studies done with caldesmon fragments have reported that each of the four domains retains most of its functional properties when separated from the rest of the molecule. Experiments have determined that most of the regulatory functions of caldesmon are contained in domain

4b, the carboxyl terminal 99 amino acids (Bartegi et al., 1990; Redwood and Marston, 1993). It has also been shown that this fragment of caldesmon can regulate smooth muscle filaments in a way analogous to that of TnI in striated muscles (Fraser and Marston, 1995; Marston et al., 1994a). However, this 99-residue fragment does not bind appreciably to tropomyosin, suggesting that other regions of caldesmon are responsible for structural interactions with tropomyosin (Huber et al., 1995; Redwood and Marston, 1993).

Although caldesmon has been extensively studied, the only structural information available about caldesmon and its various complexes comes from several electron microscopy (EM) studies. Rotary shadowing EM studies of single caldesmon molecules revealed an elongated shape approximately 76–80 nm long (Mabuchi and Wang, 1991). Some negatively stained thin filaments have also been studied, with EM apparently showing caldesmon wound around the actin helix (Moody et al., 1990). A more recent study also examined the structure of negatively stained native thin filaments from smooth muscle using EM (Vibert et al., 1993). Although they could not directly visualize caldesmon, they did not observe any projections away from the thin filament, suggesting that caldesmon is in close association with the thin filament along its entire length, leading to models in which caldesmon and tropomyosin are bound side by side (Marston and Redwood, 1991; Moody et al., 1990; Watson et al., 1990b). They also noted that the position of tropomyosin was shifted away from the myosin-binding sites on actin without calcium. The results of another set of EM studies also suggest that both ends of caldesmon interact with native thin filaments (Mabuchi et al., 1993). Last year, additional structural studies were published showing that only domain 4 of caldesmon (the carboxyl-terminal fragment) bound tightly to reassembled tropomyosin:actin filaments and that domains 1 and 2 projected away from the thin filament under some conditions (Katayama and Ikebe, 1995). Other studies have found that reassembled thin filaments are indistinguishable from native thin filaments (Hodgkinson et al., unpublished data).

A series of fluorescence and affinity chromatography studies with fragments of both caldesmon and tropomyosin have also been used to identify which pieces interact (Huber et al., 1995; Redwood and Marston, 1993; Tsuruda et al., 1995; Watson et al., 1990a,b). Several of these studies have also suggested that caldesmon:tropomyosin-binding sites are discrete but extended (Huber et al., 1995; Watson et al., 1990b). The results of these studies suggest that almost every region of caldesmon can bind to some part of tropomyosin under certain conditions and that the carboxyl-terminal domain of caldesmon contains a strong tropomyosin-binding site.

In this paper the first detailed three-dimensional structural information about the interactions of caldesmon and tropomyosin determined using x-ray crystallography is reported. The binding of both full-length and several fragments of caldesmon to tropomyosin has also been examined using an evanescent wave optical biosensor in an attempt to quantify the binding specificity and strength of each caldesmon domain.

MATERIALS AND METHODS

Protein purification

Skeletal $\alpha\alpha$ tropomyosin was purified from rabbit skeletal muscle by previously published methods (Whitby et al., 1992; White et al., 1987). Chicken skeletal $\alpha\alpha$ and gizzard $\alpha\beta$ tropomyosins were purified using the same basic procedure. Unacetylated chicken skeletal tropomyosin was expressed in bacteria and purified as previously reported (Hitchcock-DeGregori and Heald, 1987). Bovine serum albumin (BSA) was purchased from Sigma Chemical Co.

All caldesmon fragments are based on the sequence of chicken gizzard caldesmon (Bryan et al., 1989). CaD-1 (residues 1–128) and CaD-2 (230–419) were expressed as described by Redwood and Marston (1993). Full-length caldesmon was purified from chicken gizzard according to the method of Lynch and Bretscher (1986). Caldesmon fragments CaD-4 (597–756) and CaD-3 (413–579), were generated by recombinant methods and expressed in *E. coli* using a T7-promoter-based expression vector pAED4. CaD-4 was purified using a slight variation of a previously published procedure (Wang et al., 1991). Briefly, the bacterial cell extracts were first heated at 100°C for 15 min, followed by centrifugation; the supernatant was loaded onto a calmodulin-affinity column in the presence of Ca^{2+}. After washing with Ca^{2+} buffer, the bound fractions were eluted from the column with an EDTA-containing buffer; the CaD fragment thus obtained was further purified on a DE-52 ion exchange column. CaD-3 was purified by a similar procedure (J. Kordowska, unpublished observation). Briefly, the bacterial extract was heated and spun as above, and the supernatant was first applied to a DE-52 column at pH 7. CaD-3 did not bind and was collected in the flow-through fractions. After the pH was adjusted to 5, the pooled fractions were loaded onto a CM-52 cation exchange column equilibrated at pH 5. CaD-3 was then eluted from the column with a salt gradient. MG56C (658–713) was purified from *E. coli* as described (Zhuang et al., 1995). Recombinant chicken brain calmodulin (CaM) was purified from *E. coli* by phenyl-Sepharose column chromatography (Dedman and Kaetzel, 1983). Protein concentrations were determined spectrophotometrically using the following molar extinction coefficients ($cm^{-1}\ M^{-1}$): tropomyosin, 15,800 at 277 nm; whole caldesmon, 28,990 at 280 nm; CaD-4, 8600 at 280 nm; CaD-3, 5600 at 280 nm; MG56C, 11,200 at 280 nm; CaM, 3300 at 277 nm. Protein concentrations for CaD-1 and CaD-2 were estimated using the Lowry method (Lowry et al., 1951).

Crystallization

Tropomyosin crystals (Bailey, 1948) were grown in capillary tubes by liquid-liquid diffusion as previously described (Chacko and Phillips, 1992; Phillips, 1985). The protein concentration was 10 and 12 mg/ml, and the pH was between 5.6 and 5.9 in 100 mM NaCl and 50 mM ammonium sulfate. These crystals are composed of tropomyosin filaments connected head to tail, running parallel to the body diagonal of the unit cell (space group $P2_12_12$ with a = 120 Å, b = 240 Å, c = 300 Å). The crystals are greater than 95% solvent, which limits diffraction resolution to around 15 Å. However, the open mesh formed by the tropomyosin filaments provides ample space to soak other proteins into the crystal lattice, such as troponin and caldesmon, which can then bind to the tropomyosin filaments. Because Bailey crystals are extremely fragile as grown, the crystals were lightly cross-linked with 0.1% glutaraldehyde to stabilize them. In earlier work with troponin, this treatment was shown not to affect the interactions of troponin and tropomyosin (White et al., 1987). Earlier studies examining troponin binding to Bailey tropomyosin crystals were done with the tropomyosin crystals as grown, at pH ~5.8 and an ionic strength of about 150 mM (White et al., 1987). However, caldesmon binding to tropomyosin is reported to be ionic strength dependent and varies with pH (Marston and

Redwood, 1991). For these studies with caldesmon, the pH of the crystals was gradually changed to pH 7 and the ionic strength was lowered to 30–60 mM imidazole before whole caldesmon or fragments were then layered onto the crystal and allowed to diffuse into the crystal for several hours before x-ray data were collected.

Data collection and processing

X-ray diffraction data were collected on a Siemens area detector, rotating anode system equipped with Franks double focusing mirrors to obtain a finely focused beam. The detector-to-crystal distance was 295 mm, and a helium path was used to minimize air scattering of X-rays. The beam stop was made as small as possible and was suspended on a thin strip of mylar a few millimeters from the detector surface to allow the collection of low-resolution reflections. The Bailey crystals are fragile and deteriorate slowly at room temperature, so the data were collected at about 4°C; a stream of cold air was used to cool the crystal. For a typical crystal several hundred 200–400-s frames were collected as 0.2–0.4° oscillations. The data were processed using the XDS software package (Kabsch, 1988). The co-crystals diffracted x-rays to 16–20-Å resolution (Table 1). Whole caldesmon and native tropomyosin data sets were collected from single crystals. Data from the two diffraction experiments with CaD-4 were scaled and merged using the program XSCALE (Kabsch, 1988).

Difference maps and phase refinement

Initial phases for the co-crystal electron density maps were based on pure tropomyosin phases and were improved by solvent flattening and figure-of-merit weighting (White et al., 1987). The Bailey crystals are greater than 95% solvent, so the initial maps were multiplied by a mask with values of 0 in most of the solvent region and values of 1 at and around the tropomyosin filaments with a radius of ~30 Å. The resulting map was then used to generate a new set of phases. This flattening was repeated several times until the intensity-weighted root-mean-squared difference of the phases between two cycles was less than 10°. Fourier difference maps were calculated using coefficients generated by subtracting native tropomyosin data from the caldesmon:tropomyosin data. The resulting electron density maps were visualized using the program CHAIN (Sack, 1988). Figs. 2 and 3 were generated using the program MOLSCRIPT (Kraulis, 1991).

Biosensor binding experiments

All kinetic experiments were done using an IAsys optical biosensor following the manufacturer's recommended procedures (Fisons Applied Technology, Cambridge, England). An amino coupling kit (containing 1-ethyl-3-(3-dimethylaminopropyl)carbodiimide, *N*-hydroxy-succinimide, and 1 M ethanolamine, pH 8.5) and IAsys carboxymethyl dextran (CMD) cuvettes were purchased from Fisons Applied Sensor Technology. Tropomyosin was immobilized to the CMD cuvettes, via its amino groups, as previously described for other proteins (Davies et al., 1994). Several cuvettes were treated with an average of 13 ng/mm^2 of tropomyosin immobilized to each 18-mm^2 cuvette surface. The binding (or lack of binding) of whole caldesmon and caldesmon fragments to immobilized tropomyosin was assessed. For each binding assay the cuvette was equilibrated with 200 μl of buffer (50–150 mM NaCl, 10 mM phosphate, 1 mM EDTA, 1 mM DTT, 2 mg/ml BSA, pH 7.4) for several minutes. Protein samples (2–40 μl) were then added and allowed to bind for several minutes. After the association was measured, the cuvette was emptied and filled with a fresh 200 μl of buffer, and the dissociation was followed for several minutes. Each sample was analyzed at several concentrations, and every concentration was tested at least twice.

Data were analyzed with the FASTfit software package provided with the IAsys instrument. The details of data analysis using this software have previously been described and involve a nonlinear regression fit of two integrated rate equations to the data (Davies et al., 1994; Edwards et al., 1995; George et al., 1995). Raw data were also exported and then processed using the Igor Pro software package and integrated rate equations.

On the biosensor surface the reaction between the immobilized protein (I) and the free ligate (L) can be described as a simple reversible reaction between two homogeneous species such that

$$L + I \underset{k_{diss}}{\overset{k_{ass}}{\rightleftharpoons}} LI. \quad (1)$$

The observed rate constant (k_{obs}) is defined as

$$k_{obs} = (k_{ass}[L] + k_{diss}). \quad (2)$$

In the IAsys the amount of LI (protein complex) is measured directly as the response (R) of the machine in units of arc seconds. The [IL] at equilibrium can be called the extent (E) of reaction. Thus the association of a ligate to an immobilized protein can be described by the following pseudo-first-order rate equation:

$$R_t = R_0 + E(1 - e^{-k_{obs}t}) \quad (3)$$

where R_t is the instrument response at time t and R_0 is the response immediately before the ligate is added to the cuvette. The FASTfit software uses an iterative nonlinear least-squares curve-fitting procedure to derive values of k_{obs} and E from the data. As can be seen from Eq. 2, a plot of k_{obs} against [L] should give a straight line with a y-axis intercept of k_{diss} and a slope of k_{ass}. A related equation can also be used to fit data assuming two different rate constants:

$$R_t = R_0 + E_1(1 - e^{-k_{obs(1)}t}) + E_2(1 - e^{-k_{obs(2)}t}). \quad (4)$$

RESULTS

The interactions of several caldesmon domains with tropomyosin have been examined. Structures of co-crystals of

TABLE 1 Crystal statistics for tropomyosin crystals and co-crystals

Soaked protein*	Completeness (%) to 16 Å	Unit cell (Å)			R_{sym}# (%) (all data)	R_{sym} (%) ($I > 3\sigma$)
		a	b	c		
wCaD	99.0	123.5 ×	244.5 ×	291.4	22.9	10.1
CaD-4 (data set 1)	80.8	112.7 ×	242.8 ×	300.8	19.9	10.0
CaD-4 (data set 2)	43.2	124.4 ×	239.9 ×	296.6	25.1	11.5
CaD-4 (merged data)	93.0				27.0	11.0
CaD-3	98.6	117.4 ×	238.1 ×	294.7	17.9	9.5
none	99.3	116.0 ×	240.0 ×	299.1	14.2	8.0

*Proteins soaked into Bailey tropomyosin crystals: wCaD, whole chicken caldesmon; CaD-4, caldesmon residues 597–756; CaD-3, residues 413–579; none, no additional protein.

#$R_{sym} = \Sigma_h\Sigma_i|I_{h,i} - I_h|/\Sigma_h\Sigma_i I_{h,i}$, where I_h is the intensity of reflection h, Σ_h is the sum over all reflections, and Σ_i is the sum over all i measurements of reflection h.

tropomyosin with whole caldesmon and caldesmon domain 4 (CaD-4) were determined by x-ray crystallography. The electron density maps revealed which regions of tropomyosin interacted with caldesmon and showed that several domains of caldesmon bound to tropomyosin at low ionic strength. A brief account of the crystallography results was previously reported (Hnath and Phillips, 1995). The binding of whole caldesmon and fragments to immobilized tropomyosin was measured using an optical biosensor. Only whole caldesmon and CaD-4 bound to tropomyosin with micromolar affinity under near-physiological salt conditions, whereas none of the other fragments bound specifically at 100 mM or higher salt.

Tropomyosin-caldesmon co-crystals

Whole caldesmon or fragments were layered onto tropomyosin crystals and allowed to soak into the crystals for several hours. Data were then collected of these "co-crystals" (Table 1). Although the R_{sym} for all data is high, this is due primarily to the many weakly diffracting reflections that are characteristic of the highly anisotropic diffraction patterns of these tropomyosin crystals. Earlier studies with troponin indicated visible changes in the diffraction pattern of Bailey crystals with troponin bound to them, the most obvious changes being in the OKL reflections. Comparison of diffraction patterns from tropomyosin:caldesmon co-crystals and tropomyosin:troponin co-crystals to native tropomyosin crystals showed similar changes, suggesting that caldesmon had bound inside the crystal (Fig. 1).

Structure of whole caldesmon: tropomyosin crystals

Difference Fourier maps were used to locate the position of caldesmon in the tropomyosin crystals. Because caldesmon is almost twice the length of tropomyosin, a clean map of caldesmon on the tropomyosin lattice was not anticipated. It was expected that only caldesmon's attachment site(s) on tropomyosin would be visible. The map showed that caldesmon bound tropomyosin in several places over most of the tropomyosin molecules (Fig. 2). One region of caldesmon bound close to the region where the tropomyosin filaments cross over each other, near tropomyosin residues 70–100 and residues 230–260 of the nearby molecule; another part of caldesmon bound near residues 160–210; and a final part of caldesmon interacted with tropomyosin residues 5–50. Contouring at higher levels revealed that the strongest binding site was near the tropomyosin residues 70–100 and residues 230–260 of a symmetry-related tropomyosin molecule and a slightly weaker site near tropomyosin 190–210. Caldesmon did not appear to directly bind to the head-to-tail overlap region.

Structure of CaD-4:tropomyosin co-crystals

To help define which region of caldesmon was binding to the tropomyosin crystal, data were also collected where the C-terminal portion of caldesmon (CaD-4) had been soaked into a crystal. Examination of the calculated difference map (Fig. 3 *A*) revealed some density near the cross-over region of the tropomyosin molecules. The density was in a place similar to that of the strongest binding region seen with whole caldesmon. Another difference map was calculated, subtracting the CaD-4 data set from the whole caldesmon data (Fig. 3 *B*). This map shows a density similar to that of the whole CaD-tropomyosin map, except for the density near tropomyosin residues 70–100 and residues 230–260. This confirmed that the CaD-4 fragment had bound to the tropomyosin crystal and that CaD-4 contained the strongest binding sites seen in the whole caldesmon map. However, it was still not known which other region(s) of caldesmon was responsible for the electron density seen in the whole caldesmon maps near tropomyosin 190 and near the amino terminus.

Other caldesmon domains

Earlier studies suggested that caldesmon domain 3 (CaD-3) might bind to tropomyosin, based on its 43% identity to TnT residues 89–147 and the fact that this

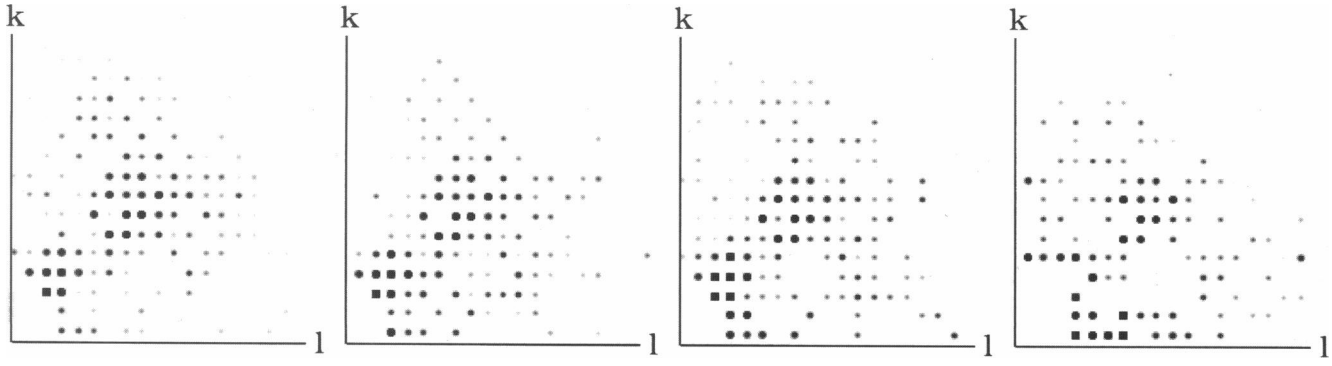

FIGURE 1 Observed diffraction data from one crystallographic plane of Bailey tropomyosin crystals. From left to right are data from crystals of pure tropomyosin, tropomyosin:troponin, tropomyosin:caldesmon, and tropomyosin:CaD-4. Unique reflections to 16 Å are shown.

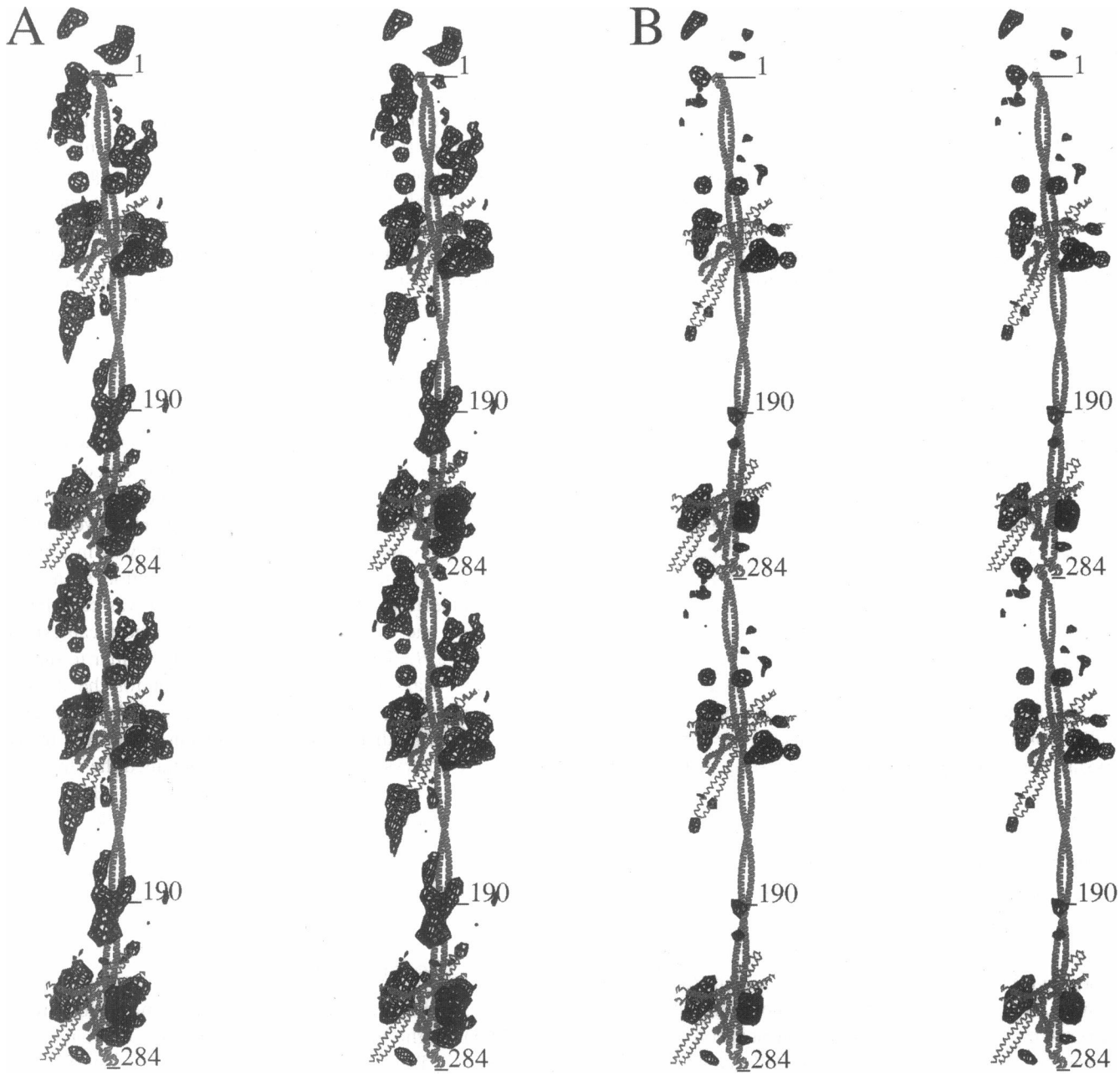

FIGURE 2 Stereo difference maps of whole caldesmon:tropomyosin crystal electron density minus pure tropomyosin showing the extra density (in black) corresponding to caldesmon in the crystal. Two overlapping tropomyosin molecules are shown with electron density within a 30-Å radius. Nearby symmetry-related tropomyosin molecules are also shown. (*A*) Difference map contoured at 2 sigma. (*B*) Map contoured at 3 sigma.

region of TnT binds to tropomyosin (Bryan et al., 1989; White et al., 1987). Therefore, several attempts were made to collect data sets with CaD-3 soaked into Bailey crystals. Significant changes in the diffraction patterns were not observed in any of these data sets. Difference maps subtracting pure tropomyosin from the tropomyosin:CaD-3 data did not reveal any significant extra density (data not shown). Furthermore, a difference map of whole caldesmon minus CaD-3 looked almost identical to the whole caldesmon minus pure tropomyosin map, confirming that CaD-3 had not bound to the crystals. At this point it was still not clear which other region of caldesmon was binding to tropomyosin in the crystals or if there were differences in the binding of caldesmon to skeletal and smooth muscle tropomyosin. Therefore it was decided to examine the binding of caldesmon domains to tropomyosin by another method.

Biosensor binding studies

The new optical biosensors based on evanescent-wave detection provide a relatively facile way to assess the affinity

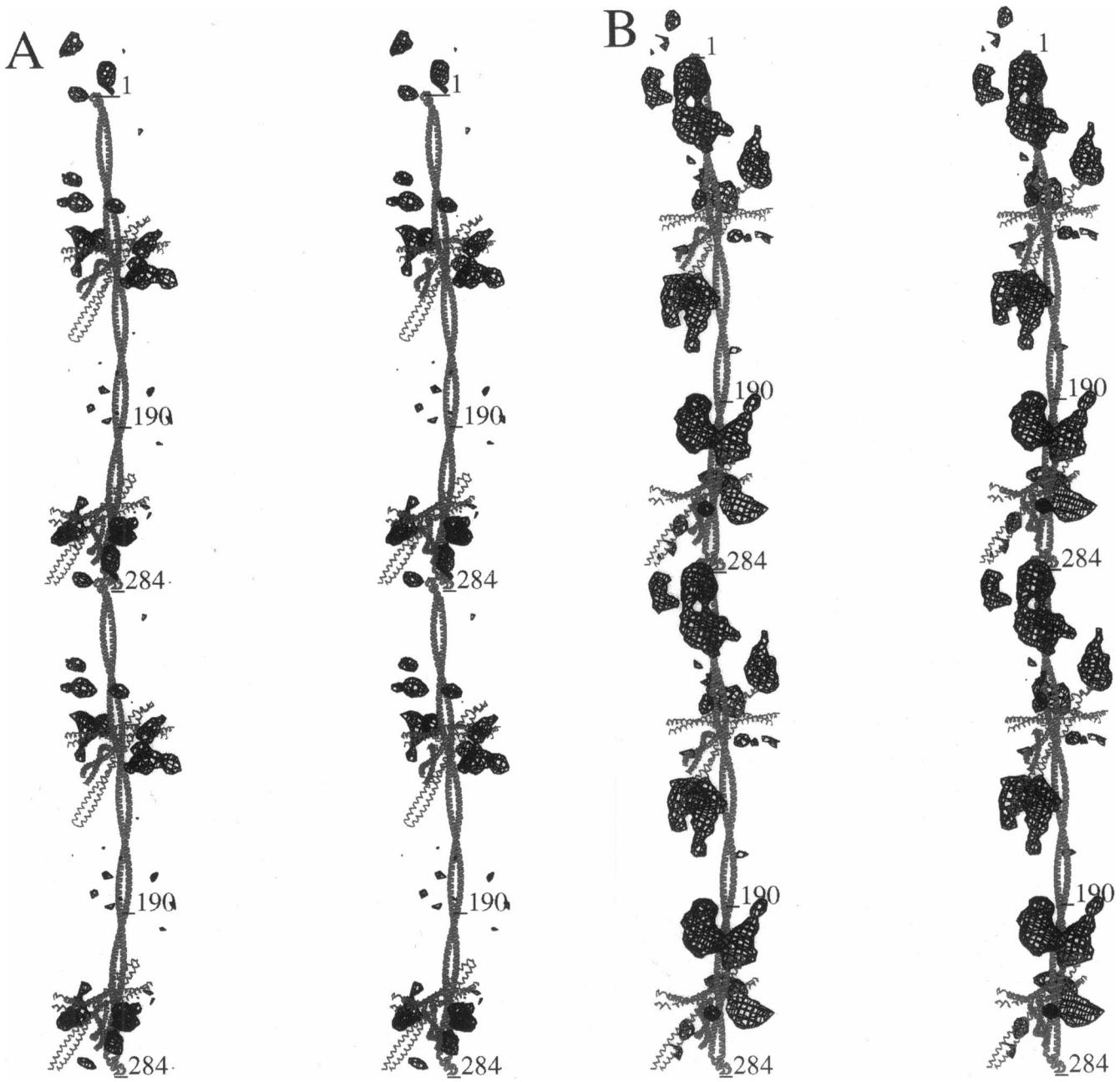

FIGURE 3 Stereo difference maps showing the binding of CaD-4 to tropomyosin in the Bailey crystal. (*A*) Difference map of a CaD-4:tropomyosin minus pure tropomyosin (contoured at 2.5 sigma). (*B*) Difference map of whole caldesmon minus CaD-4, showing that CaD-4 does indeed bind to the node region (contoured at 2.25 sigma). The remaining density seen in the second map suggests that caldesmon does have other regions, besides CaD-4, that bind to tropomyosin near tropomyosin residues 180–210 and 5–50.

of caldesmon domains for tropomyosin under a variety of conditions (Yeung et al., 1995). The use of an optical biosensor requires that one of the biomolecules be immobilized, and because the goal was to examine the binding of several fragments of caldesmon to tropomyosin, tropomyosin was immobilized. It was thought this choice might also simplify the observed kinetic data, because tropomyosin binds to itself in a head-to-tail manner.

Initial measurements of caldesmon domains binding to skeletal and smooth muscle tropomyosin were done in 150 mM NaCl, 10 mM phosphate (pH 7.4). However, the binding of most of the fragments was weak under these conditions. Binding measurements at 100 mM and 50 mM NaCl were attempted to see if binding occurred under these conditions. However, nonspecific binding (as determined by binding of caldesmon domains to immobilized myoglobin and BSA) was observed for most of the caldesmon fragments as well as for whole caldesmon. To circumvent this problem, 2 mg/ml BSA was added to all of the buffers. This experimental protocol helped in most cases, although non-

specific binding was still observed at 50 mM NaCl for some of the caldesmon domains and at caldesmon concentrations above 2 μM.

The raw data from the IAsys were processed using the FASTfit software package provided with the instrument and with the Igor Pro software package. The results obtained from both methods were indistinguishable. Two types of analysis were undertaken, providing kinetic and equilibrium binding affinities. For the kinetic analysis, values of k_{ass} and k_{diss} were derived from the data which were then used to calculate the overall affinity ($k_{diss}/k_{ass} = K_D$ (M)). The equilibrium binding affinities were calculated by plotting the extent of binding against concentration. The result is a standard equilibrium binding curve, where the K_D is the concentration required for half-maxium binding.

Whole caldesmon and CaD-4 binding to tropomyosin

The binding of several different caldesmon domains to tropomyosin was examined, but only whole caldesmon and CaD-4 bound with strong, specific affinity (Table 2). The whole caldesmon and CaD-4 binding curves indicated that equilibrium was nearly achieved in a few minutes and that the equilibrium K_D could be directly estimated in addition to calculating it as the ratio of the rate constants (Fig. 4). Some typical examples of the analysis for whole caldesmon and CaD-4 binding to tropomyosin are shown in Figs. 5 and 6. As is often observed in biosensor data, the association rate curves were biphasic, with the second phase being ~10-fold slower than the first phase. The slower phases of data from biosensor experiments with unoriented immobilized proteins are, for the most part, disregarded, as they probably represent the behavior of less than fully active protein and usually comprise less than 30% of the total binding response (Edwards et al., 1995). Unfortunately, all of the caldesmon binding curves had two phases, both ~50% of the total curve and with apparently different association and dissociation rates but similar overall affinities (Fig. 7 and Table 3). These data made it difficult to ignore the slower association rate, because it seemed to correspond to a similarly slower dissociation rate. It was difficult to see a clear pattern in the association and dissociation rates, but examination of the equilibrium affinities showed that caldesmon binding to three types of tropomyosin was similar at each salt concentration and that the affinity became looser with increasing salt (Table 3). While a highly accurate measure of K_D requires rate and binding measurements that range well above the concentration that is the K_D, nonspecific binding did not permit rounding out the data set with concentrations at the high end of the range. Thus the authors acknowledge that these measurements of K_D are only the most accurate

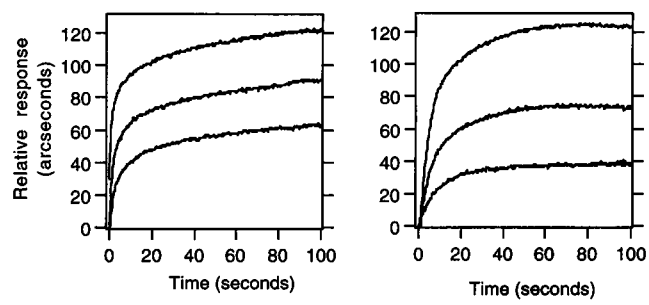

FIGURE 4 Binding of whole caldesmon (*left*) and CaD-4 (*right*) to immobilized chicken gizzard tropomyosin in 150 mM NaCl, 10 mM phosphate (pH 7.2), 1 mM DTT, 1 mM EDTA, and 2 mg/ml BSA. The concentrations shown are (from top to bottom) 1550, 775, and 387 nM for whole caldesmon and 1875, 937, and 375 nM for CaD-4. Each concentration was measured at least twice. Clearly the rate of association increases with concentration. The binding is almost complete after 100 s, at the concentrations examined, and the curve fitting software could easily extrapolate to equilibrium. Similar concentration dependencies were seen for all assays of caldesmon and CaD-4 binding to tropomyosin.

TABLE 2 Caldesmon fragments binding to tropomyosin

Ligate*	Immobilized#	NaCl (mM)	Affinity§ (M)
wCaD	rsTm	150	$0.9 \pm 0.6 \times 10^{-6}$
wCaD	cgTm	150	$1.0 \pm 0.7 \times 10^{-6}$
CaD-4	rsTm	150	$1.9 \pm 1.3 \times 10^{-6}$
CaD-4	cgTm	150	$1.5 \pm 0.5 \times 10^{-6}$
CaD-4	unTm	150	$1.5 \pm 0.7 \times 10^{-6}$
wCaD	rsTm	100	$5.6 \pm 5.1 \times 10^{-7}$
wCaD	unTm	100	$4.2 \pm 2.2 \times 10^{-7}$
CaD-4	rsTm	100	$9.2 \pm 4.6 \times 10^{-7}$
CaD-4	cgTm	100	$8.5 \pm 2.6 \times 10^{-7}$
wCaD	rsTm	50	$3.1 \pm 2.3 \times 10^{-7}$
wCaD	cgTm	50	$1.3 \pm 0.4 \times 10^{-7}$
wCaD	unTm	50	$1.5 \pm 0.4 \times 10^{-7}$
CaD-4	cgTm	50	$2.5 \pm 3.0 \times 10^{-7}$
CaD-1, CaD-2, CaD-3, MG56C	rsTm, cgTm	100, 150	Not detectable
CaD-3, MG56C	rsTm, cgTm	50	Not detectable
CaD-1, CaD-2	rsTm, cgTm	50	Not specific

*Caldesmon fragment: wCaD, whole chicken caldesmon (residues 1–756); CaD-4, residues 597–756; CaD-1, residues 1–128; CaD-2, residues 230–419; CaD-3, residues 413–579; MG56C, residues 658–713.
#Immobilized tropomyosin: rsTm, $\alpha\alpha$-rabbit skeletal; cgTm, $\alpha\beta$-chicken gizzard; unTm, $\alpha\alpha$-unacetylated chicken skeletal.
§Affinity calculated from equilibrium data.

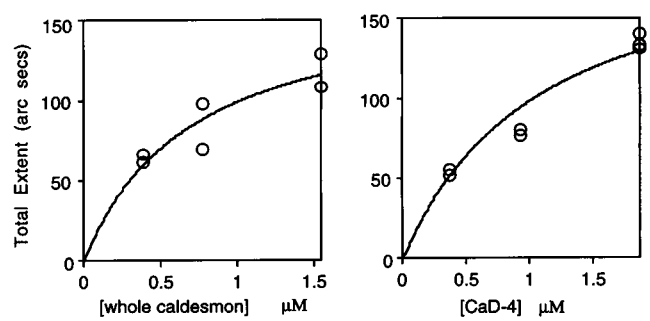

FIGURE 5 Equilibrium binding analysis of whole caldesmon and CaD-4 interacting with immobilized tropomyosin. Extrapolated binding extents were plotted against whole caldesmon (*left*) and CaD-4 (*right*) concentration. The line is calculated from the binding constant providing the best fit for the data. The results of all of the curve fitting analyses are summarized in Table 2.

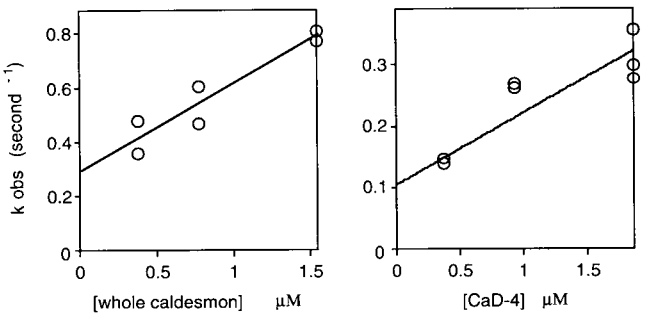

FIGURE 6 Kinetic analysis of the binding of whole caldesmon and CaD-4 to immobilized tropomyosin. The observed association rates (k_{obs}) for the binding of caldesmon to tropomyosin were obtained by curve fitting the association curves shown in Fig. 4. The results were plotted against caldesmon concentration. The slope of this line is the k_{on} (association rate), and the y-intercept is the k_{off} (dissociation rate). The results of these plots and all other kinetic analyses are shown in Table 3.

estimates technically possible for these proteins under these conditions.

Regulation by calmodulin/calcium

The effect of CaM/Ca^{2+} on the interaction of tropomyosin and caldesmon was also examined. While collecting the CaD-4:tropomyosin kinetic data, instead of simply measuring the dissociation rate, in some experiments we added fivefold molar excess of calmodulin to the CaD-4 buffer in the cuvette after the binding curve appeared to be saturated. The result was dramatic; CaD-4's affinity for tropomyosin was quickly reduced, with greater than 90% of the CaD-4 dissociating in less than 10 s (Fig. 8). Adding excess EDTA to the cuvette reversed the effect, allowing CaD-4 to bind to tropomyosin, again resulting in another binding curve. Similar results were seen for whole caldesmon and the addition of Ca^{2+}/calmodulin to the cuvette before the addition of caldesmon or CaD-4 completely inhibited the binding of whole caldesmon and CaD-4 to tropomyosin.

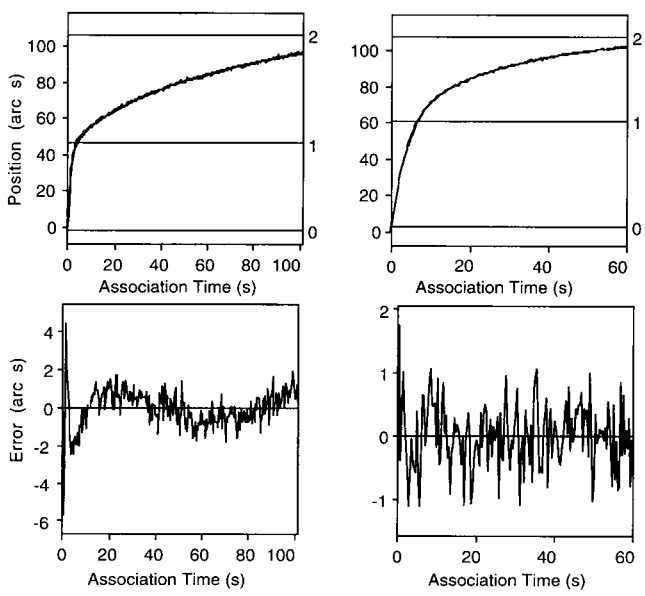

FIGURE 7 Curve fitting of whole caldesmon (*left*) and CaD-4 (*right*) binding to tropomyosin. For the top figures the IAsys response is shown on the left axes and the calculated biphasic binding extents are shown on the right. Notice that in both cases each extent makes up approximately 50% of the total binding. Although the binding of CaD-4 seems to be fairly well described by a double exponential equation, the binding of whole caldesmon appears to be multiphasic and is not even fit well, assuming a two-site attachment.

Different tropomyosins

The binding of caldesmon to different tropomyosins was examined. Although most of the experiments were done with rabbit skeletal tropomyosin, caldesmon binding to chicken gizzard tropomyosin and to unacetylated chicken skeletal tropomyosin (which cannot polymerize head to tail like native muscle tropomyosin) was also measured under some conditions. The affinity of whole caldesmon and CaD-4 for all three tropomyosins was similar for the conditions examined (Tables 2 and 3).

DISCUSSION

The interactions of whole caldesmon and several domains of caldesmon with tropomyosin have been examined. Only whole caldesmon and CaD-4 bound specifically to either skeletal, smooth, or unacetylated tropomyosin at ionic strengths above 100 mM. Because specific strong binding of other fragments by either crystallography or biosensor technology could not be detected, it appears that if other domains of caldesmon do bind to tropomyosin, they do so weakly and/or only when held close to tropomyosin by domain 4.

Caldesmon and tropomyosin interactions

These results are consistent with work from earlier studies that suggest that caldesmon can bind along the length of tropomyosin (Moody et al., 1990; Vibert et al., 1993; Watson et al., 1990a). EM experiments have previously shown that caldesmon binds to native thin filaments in a lengthwise fashion (Mabuchi et al., 1993). Furthermore, these present results confirm the hypothesis that caldesmon: tropomyosin-binding sites are discrete but extended (Redwood and Marston, 1993; Watson et al., 1990b). The regions of caldesmon that interact with tropomyosin have been studied by several groups over the years. The results of earlier studies indicated that caldesmon domains 2 and 4 bound to tropomyosin with the highest affinity (Redwood and Marston, 1993). A more detailed mapping of the residues in domains 3 and 4 of human caldesmon that interact with tropomyosin has recently been reported, and it was concluded that the strong tropomyosin-binding site is located in region 4a, but that domain 3 can bind to skeletal,

TABLE 3 Kinetic data for whole caldesmon and CaD-4 binding to tropomyosin

Ligate*	Immob	NaCl (mM)	k_{on1}[#] ($M^{-1}s^{-1}$) × 10^3 k_{off1} (s^{-1})	k_{on2} ($M^{-1}s^{-1}$) × 10^3 k_{off2} (s^{-1})	K_{D1}[§] (μM) K_{D2}	K_{Deq}[¶] (μM)
wCaD	rsTm	150	320 ± 100 0.20 ± 0.13	4.9 ± 6.6 0.014 ± 0.008	0.62 ± 0.58 2.87 ± 5.54	0.86 ± 0.57
wCaD	cgTm	150	300 ± 110 0.29 ± 0.16	12 ± 4.3 0.0055 ± 0.0050	0.97 ± 0.89 0.44 ± 0.55	1.02 ± 0.74
CaD-4	r sTm	150	61 ± 7.8 0.070 ± 0.035	5.5 ± 6.2 0.0045 ± .0018	1.15 ± 0.72 0.82 ± 1.25	1.85 ± 1.30
CaD-4	cgTm	150	120 ± 19 0.10 ± 0.02	15 ± 5.8 0.015 ± 0.006	0.86 ± 0.31 1.01 ± 0.80	1.13 ± 0.56
CaD-4	unTm	150	68 ± 46 0.10 ± 0.11	6.7 ± 3.9 0.014 ± 0.009	1.48 ± 2.64 2.08 ± 2.53	1.40 ± 0.68
wCaD	rsTm	100	63 ± 25 0.045 ± 0.020	ND[‖]	0.71 ± 0.60	0.56 ± 0.51
wCaD	unTm	100	160 ± 91 0.036 ± 0.080	ND	0.23 ± 0.63	0.42 ± 0.22
CaD-4	rsTm	100	51 ± 8.4 0.026 ± 0.0069	8.7 ± 3.3 0.0066 ± 0.0027	0.51 ± 0.22 0.76 ± 0.60	0.92 ± 0.46
CaD-4	cgTm	100	14 ± 3.3 0.051 ± 0.0029	2.3 ± 1.3 0.0089 ± 0.0011	3.60 ± 1.04 3.84 ± 2.58	0.85 ± 0.26
wCaD	rsTm	50	ND	ND		0.31 ± 0.23
wCaD	cgTm	50	ND	ND		0.13 ± 0.04
wCaD	unTm	50	380 ± 81 0.079 ± 0.020	31 ± 14 0.0071 ± 0.0033	0.21 ± 0.10 0.23 ± 0.21	0.15 ± 0.04
CaD-4	cgTm	50	ND	ND		0.25 ± 0.30

*Ligates and immobilized proteins are as described in Table 2.
[#]k_{on} are the association rate constants as derived from the slope of plots like Fig. 6. k_{off} are the dissociation rate constants as derived from the intercept of plots like Fig. 6. k_{on1} and k_{on2} represent the values derived from the first phase and the second phase of a biphasic fit of the data.
[§]Affinity calculated by dividing the k_{off} by the k_{on}.
[¶]Affinity calculated from equilibrium data.
[‖]Not determinable because of either the absence of a second phase or the inability to fit the data in a congruous manner.

but not smooth, tropomyosin at low ionic strength (Huber et al., 1995). Some recent EM studies have also shown that the carboxyl-terminus of caldesmon contains the strong binding site for tropomyosin (Katayama and Ikebe, 1995), whereas another laboratory, using a number of caldesmon C-terminal deletion mutants, has proposed a tropomyosin-binding site in domain 4b (residues 717–727) of caldesmon (Wang et al., 1996). The results of a series of cross-linking experiments with caldesmon, tropomyosin, and actin also suggest that the amino-terminal domain of caldesmon does not interact with actin or tropomyosin in reconstituted thin filaments (Graceffa, 1995).

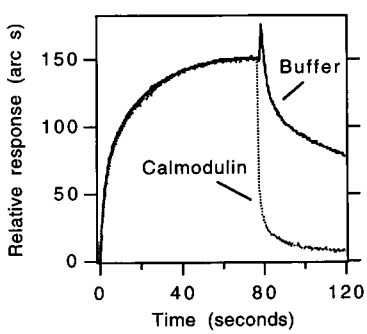

FIGURE 8 Binding and dissociation of CaD-4 to immobilized skeletal tropomyosin in the presence and absence of calmodulin. CaD-4 was allowed to bind to tropomyosin in the same buffer described in Fig. 4 except for the addition of 2 mM calcium. The cuvette was then either emptied and filled with fresh buffer, or a fivefold molar excess of calmodulin was added.

The region of tropomyosin that interacts with caldesmon has also been investigated over the years. Studies using affinity chromatography, fluorescently labeled proteins, and competition assays found that tropomyosin residues 142–227 have the strongest interaction with caldesmon (Tsuruda et al., 1995; Watson et al., 1990b). It was also shown that tropomyosin 11–127 binds caldesmon, but with less affinity and only in the absence of actin. Furthermore, strong binding of both caldesmon 1–152 and caldesmon 443–736 to tropomyosin has been reported (Tsuruda et al., 1995). The results presented in this paper confirm that the C-terminal domain of caldesmon does bind tropomyosin, but that a different region of tropomyosin (70–100 and 230–260) interacts with caldesmon tightly. It should be noted that these studies are direct measurements of intact tropomyosin molecules, whereas the 142–227 assignment is based on the properties of tropomyosin fragments. Because this current study did not examine any caldesmon fragments that included caldesmon 129–229, it is possible that another strong tropomyosin-binding site requires these residues. If

this were so, it could account for the reported binding of caldesmon near tropomyosin 142–227. The density seen near tropomyosin 180–210 and 5–50 in the difference maps in Fig. 3 may correspond to the binding of caldesmon domains 1 or 3. It is difficult to reconcile the results of these x-ray results and the previous solution studies. It is possible that the studies using fragments of tropomyosin might not accurately reflect the binding of caldesmon to whole tropomyosin molecules joined head to tail and bound on an actin filament. It is also possible that the strong binding sites observed in the tropomyosin crystals are an artifact of the crystal packing, where some caldesmon regions may appear more prominent in the difference maps because of their interactions with several nearby tropomyosin molecules. However, this explanation is unlikely because of the extremely high solvent content of the tropomyosin crystals used and the amount of motion known to occur within these crystals (Chacko and Phillips, 1992).

Biosensor data analysis

Although real time optical evanescence biosensing is a relatively new technology, it has already been successfully used to measure the interactions of a wide variety of proteins (Szabo et al., 1995; Yeung et al., 1995). In most cases the biosensor-determined affinities are similar to the affinities reported with other methods, although there are some situations where the affinities are not directly comparable. Data from these new biosensors can be used to extract accurate association and dissociation rate constants for simple bimolecular interactions and even for some cases where the kinetics involve two separate rates for both association and dissociation. However, there are also some situations where biosensors cannot accurately extract association and dissociation rate constants unless a model for the interaction is known and incorporated into the kinetic analysis (Morton et al., 1995). These limitations were not obvious to us when the biosensor data collection began, but it became apparent that some of the data that were collected for the binding of caldesmon to immobilized tropomyosin could not be described as a simple bimolecular interaction.

There are several possible reasons why the biosensor data were difficult to analyze. First, the method used to immobilize tropomyosin probably resulted in multiple conformations with differing accessibilities of caldesmon binding sites. Although this scenario does not usually present a major difficulty in the analysis of biosensor data (Edwards et al., 1995), in this case it may be problematic, because the interactions between caldesmon and tropomyosin are primarily electrostatic and may also require tropomyosin to be in an elongated, near-linear state as it is found in muscle. A second complication for whole caldesmon is that several regions of caldesmon may bind to tropomyosin, resulting in a combination of heterogeneous immobilization and multiple binding sites that is difficult to model accurately. One final difficulty that was encountered was in the direct measurement of the dissociation phase. Considerable rebinding was observed, which is not uncommon. However, the usual remedy of adding an excess amount of the immobilized protein to the dissociation buffer was not possible because the muscle tropomyosins self-polymerized and bound to the immobilized tropomyosin on the biosensor cuvette. Some dissociation rates were measured directly when unacetylated tropomyosin was immobilized to the cuvetttes. These directly measured rates were compared to the rates derived from the kinetic analysis, and they agreed with each other within 30%. Thus the authors feel justified in using the dissociation rates of caldesmon from the other tropomyosins derived only through kinetic analysis of the data (Table 3). Overall the dissociation rates appear to decrease with decreasing salt. A fairly accurate estimation of overall affinity of whole caldesmon and CaD-4 for tropomyosin was obtainable by comparing the equilibrium and kinetic data.

The authors realize that the errors are large for many of the kinetic rates, probably because the results of multiple experiments using different preparations of caldesmon and tropomyosin were averaged. Some user error is probably also included, because these data were collected with a machine that required manual pipetting of each protein sample into the cuvette. A more accurate determination of the rate constants could be determined using a more uniform protein source and an automated biosensor. The individual K_D's calculated from either the first or second on and off rates are close to the equilibrium affinities and probably differ because they represent only a part of the total binding. As expected, the affinity of caldesmon for tropomyosin was weaker at higher salt. It was also noticed that the affinity of CaD-4 for tropomyosin seemed to be slightly less than the affinity of whole caldesmon. The inability to extract rate constants for the second phase of some experiments and at low salt may be due to a greater contribution of nonspecific binding to the raw data. Overall, the kinetic data seem to follow the patterns mentioned above, but there are a few numbers that deviate. The reason for these unusual rates is not clear but is under investigation.

Caldesmon's affinity for tropomyosin

The affinities of whole caldesmon and CaD-4 for tropomyosin reported here are similar, but slightly stronger than previously measured affinities determined by fluorescence experiments (Table 4). However, there is considerable variability in the reported affinities, which seems to be due to the use of different fluorescent labels and different buffer conditions. In particular, the ionic strength at which the experiments are done has a great effect on the affinity (Table 4). It is also possible that the overall affinity of caldesmon for immobilized tropomyosin presented here is probably slightly less than what the actual affinity is, because some of the binding was to less than ideal binding

TABLE 4 Affinity of chicken gizzard whole caldesmon to tropomyosin as determined by various methods

Method*	Salt (mM)	pH	Affinity (nM)	Reference
ANM-Tm	10 NaCl	7.0	129–333	Watson et al., 1990a
"	50 NaCl	"	1000	"
Pyrene-CaD	0	7.2	45	Watson et al., 1990b
DNS-Tm	10 KCl	7.5	25	Fujii et al., 1988
Pyrene-CaD	10 KCl	7.2	270	Horiuchi and Chacko, 1988
"	20 KCl	"	588	"
"	40 KCl	"	3300	"
"	100 KCl	"	>10,000	"
Pyrene-Tm	0	7.2	92	Tsuruda et al., 1995
Pyrene-Tm	30 KCl	7.2	400	Huber et al., 1995
IAsys	50 NaCl	7.4	150	This paper
"	100 NaCl	"	500	This paper
"	150 NaCl	"	~1000	This paper

*Type of assay: ANM-Tm, tropomyosin labeled with *N*-(1-anilinonaphthyl-4) maleimide; Pyrene-CaD, caldesmon labeled with *N*-(1-pyrenyl) maleimide; DNS-Tm, tropomyosin labeled with dansyl chloride; Pyrene-Tm, tropomyosin labeled with *N*-(1-pyrenyl) maleimide; IAsys, binding on caldesmon to unlabeled, immobilized tropomyosin.

sites. Thus it seems that the affinity of whole caldesmon for tropomyosin may be greater than has been previously estimated using fluorescence techniques, whereas the affinity of many isolated domains may be less.

The effect of Ca^{2+}/calmodulin on the affinity of caldesmon and CaD-4 for tropomyosin was also examined. The interaction of caldesmon and tropomyosin is known to be regulated by the binding of Ca^{2+}/calmodulin to caldesmon, which weakens the affinity of caldesmon for tropomyosin (Watson et al., 1990a). Previous studies have shown that CaD-4 contains both of caldesmon's two calmodulin-binding sites (Marston et al., 1994b; Mezgueldi et al., 1994; Zhuang et al., 1995). One of the most exciting aspects of optical biosensors is their ability to examine protein-ligand interactions in real time. The addition of Ca^{2+}/calmodulin to caldesmon or CaD-4 bound to tropomyosin on the IAsys cuvette resulted in a quick release of caldesmon from tropomyosin (Fig. 8).

Nonspecific binding

Although earlier studies suggested that all four caldesmon domains bind to tropomyosin, most of those binding assays were done at 10–60 mM salt (Table 4). Several of these studies reported that binding of caldesmon to tropomyosin became weaker at higher ionic strengths, and the binding of most domains could not be easily detected at 100 and 150 mM salt using fluorescent techniques. These reports raise some questions about the physiological relevance of these interactions, particularly because caldesmon and tropomyosin appear to bind primarily through electrostatic interactions (Huber et al., 1995). No appreciable specific binding of CaD-1, CaD-2, or CaD-3 to tropomyosin was observed at 100 and 150 mM salt. However, some nonspecific binding of CaD-1 and CaD-2 to tropomyosin, myoglobin, and BSA was observed at 50 mM salt. The results from other recent studies also suggest that the binding of CaD-3 and CaD-1 may not be physiologically relevant in smooth muscle, because CaD-3 only binds to skeletal and nonmuscle tropomyosin but not smooth muscle tropomyosin, and CaD-1 may only binds tropomyosin in the absence of actin (Huber et al., 1995; Lamb et al., 1996; Tsuruda et al., 1995). However, the binding of CaD-3 to tropomyosin may be important in nonmuscle caldesmon:tropomyosin interactions (Huber et al., 1995; Lamb et al., 1996). Although the second domain of caldesmon has been reported to bind to tropomyosin (Redwood and Marston, 1993), biosensor studies did not detect specific binding of CaD-2 to tropomyosin. Another laboratory has also been unable to detect binding of domain 2 of caldesmon to tropomyosin (A. Mak, personal communication). The studies undertaken here on the IAsys were carefully done with several parallel negative controls to ensure that weak, nonspecific binding was not mistaken for specific interaction.

Comparison of caldesmon to troponin

Numerous studies suggest that caldesmon may function in a manner similar to that of troponin in the regulation of muscle contraction (Fraser and Marston, 1995; Marston et al., 1994a; Marston and Smith, 1985). However, it has previously been noted that caldesmon and troponin show little similarity at the molecular level, and therefore the details of how muscle contraction is regulated by these two proteins are probably different (Marston et al., 1994a; Vibert et al., 1993). Several observations suggest that the interaction of caldesmon and tropomyosin is significantly different from the way that troponin and tropomyosin interact. The fact that caldesmon bound similarly to skeletal, smooth, and unacetylated tropomyosins, as measured with the IAsys, is one significant difference. This result confirms previous reports that caldesmon binding to tropomyosin does not appear to require the head-to-tail overlap of tropomyosin molecules (Watson et al., 1990b). On the other hand, troponin binding is highly dependent on the nature of the head-to-tail overlap and binds significantly less tightly

to unacetylated tropomyosin (which does not polymerize) than it does to polymerized tropomyosin (Pearlstone and Smillie, 1982). Another significant difference in the binding of troponin and caldesmon to tropomyosin is in the affinities of the two proteins for tropomyosin. Comparative studies with the IAsys found that caldesmon has only micromolar affinity at 150 mM salt (this paper), whereas troponin has ~100 nanomolar affinity at 150 mM salt and micromolar affinity at 500 mM salt (E. J. Hnath, unpublished results). Although caldesmon is able to regulate actin:myosin interaction through tropomyosin in vitro, it remains to be shown that this regulation occurs at a significant level in vivo (Fraser and Marston, 1995; Pfitzer et al., 1993; Taggart and Marston, 1988). Caldesmon has been shown to be able to cross-link actin and myosin filaments (Katayama et al., 1995). In this role the binding of caldesmon to tropomyosin may be important in the alignment of caldesmon on the actin filament. Caldesmon and tropomyosin have also been shown to stabilize actin filaments and prevent actin depolymerization in nonmuscle cells (Hegmann et al., 1991; Warren et al., 1994; Yamashiro-Matsumura and Matsumura, 1988). The details of how caldesmon may affect smooth muscle contraction by several different mechanisms and the roles of caldesmon in nonmuscle cells remain to be defined.

A model of caldesmon binding to tropomyosin in the thin filament

Based on results presented in this paper and previously published data, four models of how caldesmon may interact with tropomyosin in the thin filament have been constructed (Fig. 9). These models are similar to earlier models in the general arrangement of caldesmon, tropomyosin, and actin, but position caldesmon on tropomyosin at different sites (Huber et al., 1995; Tsuruda et al., 1995). All previous models have placed caldesmon on tropomyosin, assuming that the caldesmon binds most tightly to tropomyosin 170–200 and assuming an antiparallel orientation of caldesmon and tropomyosin by analogy with troponin T. It is difficult to reconcile the x-ray results of tropomyosin residues 70–100 and/or 230–260 interacting most tightly with caldesmon with the previous results. The binding of some region of caldesmon near tropomyosin 170–200 is encouraging. This suggests that these x-ray results may be consistent with the earlier solution studies, but that for some reason the tighter binding of CaD-4 to tropomyosin 70–100 and/or 230–260 was not detected earlier. It is possible that the previous studies with fragments of tropomyosin may not accurately reflect the binding of an elongated caldesmon molecule to tropomyosin filaments. It should also be

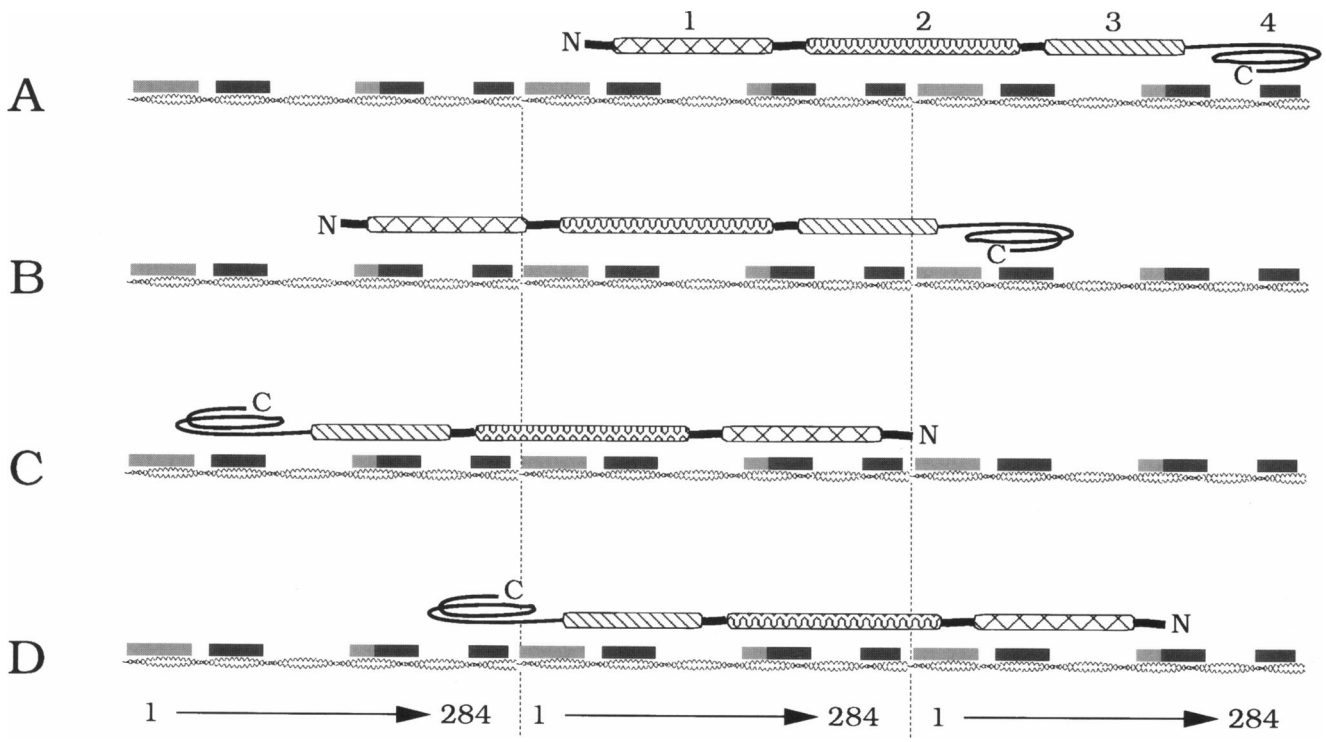

FIGURE 9 Several possible models of caldesmon and tropomyosin interactions in smooth muscle thin filaments. Three tropomyosin molecules are shown in each model, and the domain structure of caldesmon is depicted as previously proposed (Marston and Redwood, 1991). Areas of tropomyosin where caldesmon appeared to be in close association, as observed in the x-ray data difference maps, are highlighted in gray. Dark gray indicates the strongest binding sights and lighter gray shows the weaker contacts. (*A*) Model with tropomyosin and caldesmon in a parallel orientation with the C-termini of both molecules almost aligned. (*B*) Another model with tropomyosin and caldesmon aligned parallel, but with the caldesmon domain 4 aligned with tropomyosin residues 70–100. (*C*) Caldesmon and tropomyosin in an antiparallel orientation, with the C-terminus of caldesmon aligned with tropomyosin 70–100. (*D*) A second antiparallel model, with the C-termini of caldesmon and tropomyosin approximately aligned.

pointed out that because these studies did not include actin and because both tropomyosin and caldesmon bind to actin, these models may not accurately depict the interactions between these proteins that occur in muscle tissue. However, we have tried to incorporate and integrate information about caldesmon-tropomyosin-actin interactions from a variety of other studies into these models, and as such, they represent that most probable arrangements, given the current state of knowledge.

In the tropomyosin crystal a caldesmon molecule may not bind in an elongated fashion along two adjacent tropomyosin molecules as it is depicted in the model. Thus it is possible that a single caldesmon molecule may wind through the crystal, contacting several tropomyosin molecules that are in close proximity but are not joined head to tail. It is also possible that only the C-terminal domain of caldesmon may be bound to every single tropomyosin molecule and that the N-terminus may be unattached. Because there is no way of knowing the actual arrangement of caldesmon molecules within the crystal, the x-ray data can only be used to reveal the regions of tropomyosin that are in close contact with caldesmon. Furthermore, in the Bailey crystals tropomyosin molecules cross back and forth across other tropomyosin molecules. The area of closest contact between tropomyosin molecules is between residues 70–100 of one molecule and 230–260 of another tropomyosin. Unfortunately, this is also near where the tightest binding of caldesmon to tropomyosin is observed, and it is not possible to determine which region is responsible for the tight binding of caldesmon. Currently there is no direct evidence to support one model over the other, although the authors think that models B and C (Fig. 9) are more probable, because it is easier to trace longer regions of caldesmon close to tropomyosin in these models.

Many studies have been done on the structure of thin filaments in various muscle tissues. The orientation of tropomyosin on actin filaments in skeletal muscle has been defined, and it seems reasonable to assume that smooth muscle tropomyosin would bind in the same direction to smooth muscle actin filaments. Knowledge of the polarity of the actin filaments from the EM studies should also be able to define the direction of caldesmon binding to actin and could be used to construct a more accurate model of tropomyosin and caldesmon binding to the actin filament in smooth muscle. Unfortunately, myosin S-1 labeling of smooth muscle actin:caldesmon filaments has not yet clearly revealed the orientation of caldesmon to actin (E. Katayama, personal communication). It is hoped that more work will determine the polarity of caldesmon to the actin filament and tropomyosin.

Although many questions still remain about the interactions of caldesmon and tropomyosin, the results of this study and several other recent publications have helped define some of the more probable interactions (Huber et al., 1995; Katayama and Ikebe, 1995; Tsuruda et al., 1995). Caldesmon appears to be attached to tropomyosin residues 70–100 and/or 230–260 through residues 597–756. Other weaker binding sites may be located in domains 1, 2, and/or 3 of caldesmon for tropomyosin residues 180–210 and 5–50. The specific tropomyosin residues involved in the tight binding of caldesmon cannot be unambiguously determined, but based on the x-ray data they appear to be either 70–100 and/or 230–260. There may also be some regions of caldesmon that interact only weakly with tropomyosin but bind tightly to actin in muscle cells. Thus there is still much to be determined about the interactions of caldesmon and tropomyosin in smooth muscle thin filaments.

The authors thank Dr. Sarah Hitchcock-DeGregori for providing the chicken skeletal tropomyosins, Jennifer Olson for assistance with the IAsys data collection and processing, Dr. Joe Bryan for providing caldesmon, and Dr. Jim LaDine (Affinity Sensors) for his technical assistance in preparing the manuscript.

This work was supported by National Institutes of Health grants AR32764 and AR41637, National Library of Medicine grant 1T15LM07093, the Robert A. Welch Foundation, and the W. M. Keck Foundation.

REFERENCES

Allen, B. G., and M. P. Walsh. 1994. The biochemical basis of the regulation of smooth-muscle contraction. *Trends Biol. Sci.* 19:362–368.

Bailey, K. 1948. Tropomyosin: a new asymmetric protein component of the muscle fibril. *Biochem. J.* 43:271–279.

Bartegi, A., A. Fattoum, J. Derancourt, and R. Kassab. 1990. Characterization of the carboxyl-terminal 10-kDa cyanogen bromide fragment of caldesmon as an Actin-Calmodulin-binding region. *J. Biol. Chem.* 265: 15231–15238.

Bryan, J., M. Imai, R. Lee, P. Moore, R. G. Cook, and W. G. Lin. 1989. Cloning and expression of a smooth muscle caldesmon. *J. Biol. Chem.* 264:13873–13879.

Chacko, S., and G. N. Phillips, Jr. 1992. Diffuse X-ray scattering from tropomyosin crystals. *Biophys. J.* 61:1256–1266.

Dabrowska, R., A. Goch, B. Galazkiewicz, and H. Osinska. 1985. The influence of caldesmon on ATPase activity of the skeletal muscle actomyosin and bundling of actin filaments. *Biochim. Biophys. Acta.* 842:70–75.

Davies, R. J., P. R. Edwards, H. J. Watts, C. R. Lowe, P. E. Buckle, D. Yeung, T. M. Kinning, and D. V. Pollard-Knight. 1994. The resonant mirror: a versatile tool for the study of biomolecular interactions. *Tech. Protein Chem.* 5:285–292.

Dedman, J. R., and M. A. Kaetzel. 1983. Calmodulin purification and fluorescent labeling. *Methods Enzymol.* 102:1–8.

Edwards, P. R., A. Gill, D. V. Pollard-Knight, M. Hoare, P. E. Buckle, P. A. Lowe, and R. J. Leatherbarrow. 1995. Kinetics of protein-protein interactions at the surface of an optical biosensor. *Anal. Biochem.* 213:210–217.

Fraser, I. D. C., and S. B. Marston. 1995. In vitro motility analysis of smooth muscle caldesmon control of actin-tropomyosin filament movement. *J. Biol. Chem.* 270:19688–19693.

George, A. J. T., R. R. French, and M. J. Glennie. 1995. Measurement of kinetic binding constants of a panel of anit-saporin antibodies using a resonant mirror biosensor. *J. Immunol. Methods.* 183:51–63.

Graceffa, P. 1995. Cross-linking and fluorescence study of the COOH- and NH2-terminal domains of intact caldesmon bound to actin. *J. Biol. Chem.* 270:30187–30193.

Hegmann, T. E., D. L. Schulte, J. L.-C. Lin, and J. J.-C. Lin. 1991. Inhibition of intracellular granule movement by microinjection of monoclonal antibodies against caldesmon. *Cell Motil. Cytoskeleton.* 20: 109–120.

Hemric, M. E., M. V. Freedman, and J. M. Chalovich. 1993. Inhibition of actin stimulation of skeletal muscle (A1)S-1 ATPase activity by caldesmon. *Arch. Biochem. Biophys.* 306:39–43.

Hitchcock-DeGregori, S. E., and R. W. Heald. 1987. Altered actin and troponin binding of amino-terminal variants of chicken striated muscle alpha-tropomyosin expressed in *Escherichia coli*. *J. Biol. Chem.* 262: 9730–9735.

Hnath, E. J., and G. N. Phillips. 1995. Structure of co-crystals of tropomyosin and caldesmon. *Biophys. J.* 68:A163.

Huber, P. A. J., I. D. C. Fraser, and S. B. Marston. 1995. Location of smooth muscle myosin and tropomyosin binding sites in the c-terminal 288 residues of human caldesmon. *Biochem. J.* 312:617–625.

Kabsch, W. 1988. Evaluation of single-crystal x-ray diffraction data from a position-sensitive detector. *J. Appl. Cryst.* 21:916–924.

Katayama, E., and M. Ikebe. 1995. Mode of caldesmon binding to smooth muscle thin filament: possible projection of the amino-terminal domain of caldesmon from the native thin filament. *Biophys. J.* 68:2419–2428.

Katayama, E., G. Scott-Woo, and M. Ikebe. 1995. Effect of caldesmon on the assembly of smooth muscle myosin. *J. Biol. Chem.* 270:3919–3925.

Katsuyama, H., C.-L. A. Wang, and K. G. Morgan. 1992. Regulation of vascular smooth muscle tone by caldesmon. *J. Biol. Chem.* 267: 14555–14558.

Kraft, T., J. M. Chalovich, L. C. Yu, and B. Brenner. 1995. Parallel inhibition of active force and relaxed fiber stiffness by caldesmon fragments at physiological ionic strength and temperature conditions: additional evidence that weak cross-bridge binding to actin is an essential intermediate for force generation. *Biophys. J.* 68:2404–2418.

Kraulis, P. J. 1991. MOLSCRIPT: a program to produce both detailed and schematic plots of protein structures. *J. Appl. Cryst.* 24:946–950.

Lamb, N. J. C., A. Fernandez, M. Mezgueldi, J.-P. Labbe, R. Kassab, and A. Fattoum. 1996. Disruption of the actin cytoskeleton in living non-muscle cells by microinjection of antibodies to domain-3 of caldesmon. *Eur. J. Cell Biol.* 69:36–44.

Lowry, O. H., N. J. Rosebrough, A. L. Farr, and R. J. Randall. 1951. Protein measurement with the Folin phenol reagent. *J. Biol. Chem.* 193:265–275.

Lynch, W., and A. Bretscher. 1986. Purification of caldesmon. *Methods Enzymol.* 134:37–42.

Mabuchi, K., J. J.-C. Lin, and C. Wang. 1993. Electron microscopic images suggest both ends of caldesmon interact with actin filaments. *J. Muscle Res. Cell Motil.* 14:54–64.

Mabuchi, K., and C.-L. A. Wang. 1991. Electron microscopy studies of chicken gizzard caldesmon and its complex with calmodulin. *J. Muscle Res. Cell Motil.* 12:145–151.

Marston, S. B., I. D. C. Fraser, and P. A. J. Huber. 1994a. Smooth muscle caldesmon controls the strong binding interaction between actin-tropomyosin and myosin. *J. Biol. Chem.* 269:32104–32109.

Marston, S. B., I. D. Fraser, P. A. Huber, K. Pritchard, N. B. Gusev, and K. Torok. 1994b. Location of two contact sites between human smooth muscle caldesmon and Ca(2+)-calmodulin. *J. Biol. Chem.* 269: 8134–8139.

Marston, S. B., and C. S. Redwood. 1991. The molecular anatomy of caldesmon. *Biochem. J.* 279:1–16.

Marston, S. B., C. S. Redwood, and W. Lehman. 1988. Reversal of caldesmon function by anti-caldesmon antibodies confirms its role in the calcium regulation of vascular smooth muscle thin filaments. *Biochem. Biophys. Res. Commun.* 155:197–202.

Marston, S. B., and C. W. J. Smith. 1985. The thin filaments of smooth muscles. *J. Muscle Res. Cell Motil.* 6:669–708.

Mezgueldi, M., J. Derancourt, B. Calas, R. Kassab, and A. Fattoum. 1994. Precise identification of the regulatory f-actin and calmodulin-binding sequences in the 10-kDa carboxyl-terminal domain of caldesmon. *J. Biol. Chem.* 269:12824–12832.

Moody, C., W. Lehman, and R. Craig. 1990. Caldesmon and the structure of smooth muscle thin filaments: electron microscopy of isolated thin filaments. *J. Muscle Res. Cell Motil.* 11:176–185.

Morton, T. A., D. G. Myszka, and I. M. Chaiken. 1995. Interpreting complex binding kinetics from optical biosensors: a comparison of analysis by linearization, the integrated rate equation, and numerical integration. *Anal. Biochem.* 227:176–185.

Pearlstone, J. R., and L. B. Smillie. 1982. Binding of troponin-T fragments to several types of tropomyosin. *J. Biol. Chem.* 257:10587–10592.

Pfitzer, G., C. Zeugner, M. Troschka, and J. M. Chalovich. 1993. Caldesmon and a 20-kDa actin-binding fragment of caldesmon inhibit tension development in skinned gizzard muscle fiber bundles. *Proc. Natl. Acad. Sci. USA.* 90:5904–5908.

Phillips, G. N. J. 1985. Crystallization in capillary tubes. *Methods Enzymol.* 114:128–131.

Redwood, C. S., and S. B. Marston. 1993. Binding and regulatory properties of expressed functional domains of chicken gizzard smooth muscle caldesmon. *J. Biol. Chem.* 268:10969–10976.

Sack, J. S. 1988. CHAIN—a crystallographic modeling program. *J. Mol. Graph.* 6:244–245.

Smith, C. W. J., K. Pritchard, and S. B. Marston. 1987. The mechanism of Ca^{2+} regulation of vascular smooth muscle thin filaments by caldesmon and calmodulin. *J. Biol. Chem.* 262:116–122.

Sobue, K., Y. Muramoto, M. Fujita, and S. Kakiuchi. 1981. Purification of a calmodulin-binding protein from chicken gizzard that interacts with F-actin. *Proc. Natl. Acad. Sci. USA.* 78:5652–5655.

Szabo, A., L. Stolz, and R. Granzow. 1995. Surface plasmon resonance and its use in biomolecular interaction analysis (BIA). *Curr. Opin. Struct. Biol.* 5:699–705.

Taggart, M. J., and S. B. Marston. 1988. The effects of vascular smooth muscle caldesmon on force production by "desensitized" skeletal muscle fibres. *FEBS Lett.* 242:171–174.

Tsuruda, T. S., M. H. Watson, B. Foster, J. J. J.-C. Lin, and A. S. Mak. 1995. Alignment of caldesmon on the actin-tropomyosin filaments. *Biochem. J.* 309:951–957.

Vibert, P., R. Craig, and W. Lehman. 1993. Three-dimensional reconstruction of caldesmon-containing smooth muscle thin filaments. *J. Cell Biol.* 123:313–321.

Wang, C.-L. A., L.-W. C. Wang, S. Xu, R. C. Lu, V. Saavedra-Alanis, and J. Bryan. 1991. Localization of the calmodulin and the actin-binding sites of caldesmon. *J. Biol. Chem.* 266:9166–9172.

Wang, Z., K. Y. Horiuchi, and S. Chacko. 1996. Characterization of the functional domains on the C-terminal region of caldesmon using full-length and mutant caldesmon molecules. *J. Biol. Chem.* 271:2234–2242.

Warren, K. S., J. L.-C. Lin, D. D. Wamboldt, and J. J.-C. Lin. 1994. Overexpression of human fibroblast caldesmon fragment containing actin-, Ca^{2+}/calmodulin-, and tropomyosin-binding domains stabilizes endogenous tropomyosin and microfilaments. *J. Cell Biol.* 125: 359–368.

Watson, M. H., A. E. Kuhn, and A. S. Mak. 1990a. Caldesmon, calmodulin and tropomyosin interactions. *Biochim. Biophys. Acta.* 1054:103–113.

Watson, M. H., A. E. Kuhn, R. E. Novy, J. J.-C. Lin, and A. S. Mak. 1990b. Caldesmon-binding sites on tropomyosin. *J. Biol. Chem.* 265: 18860–18866.

Whitby, F. G., H. Kent, F. Stewart, M. Stewart, X. Xie, V. Hatch, C. Cohen, and G. N. Phillips Jr. 1992. Structure of tropomyosin at 9 angstroms resolution. *J. Mol. Biol.* 227:441–452.

White, S. P., C. Cohen, and G. N. Phillips, Jr. 1987. Structure of cocrystals of tropomyosin and troponin. *Nature.* 325:826–828.

Yamashiro-Matsumura, S., and F. Matsumura. 1988. Characterization of 83-kilodalton nonmuscle caldesmon from cultured rat cells: stimulation of actin binding nonmuscle tropomyosin and periodic localization along microfilaments like tropomyosin. *J. Cell Biol.* 106:1973–1983.

Yeung, D., A. Gill, C. H. Maule, and R. J. Davies. 1995. Detection and quantification of biomolecular interactions with optical biosensors. *Trends Anal. Chem.* 14:49–56.

Zhuang, S., E. Wang, and C.-L. A. Wang. 1995. Identification of the functionally relevant calmodulin binding site in smooth muscle caldesmon. *J. Biol. Chem.* 270:19964–19968.